Arab J Sci Eng (2018) 43:1709–1719
https://doi.org/10.1007/s13369-017-2728-3

RESEARCH ARTICLE - CIVIL ENGINEERING

Stability Analysis and Failure Forecasting of Deep-Buried Underground Caverns Based on Microseismic Monitoring

Jie Xu[1,2] · **Jingdong Jiang**[3] · **Quansheng Liu**[4] · **Yufeng Gao**[1,2]

Received: 21 October 2016 / Accepted: 13 July 2017 / Published online: 20 July 2017

Abstract The stability of underground caverns subjected to unloading disturbance is very important for engineering practice during construction stages. The rocks in the Xinzhuangzi Coalmine in Huainan are becoming increasingly unstable with the advancement of the excavation face. To evaluate the stability and failure mechanism of the surrounding rock mass, a microseismic (MS) monitoring system was employed to round-the-clock monitor the microseismic activities in the 62nd mining area. This MS-monitoring system was used to obtain the relationship between the MS activities and the excavation schedule. The potential risk zone of the surrounding rock mass was determined according to the temporospatial distribution law of the MS events. To reveal the instability mechanism of the potential risk zone, the seismic source parameters of the MS clusters were analyzed. The results show that the deformation and failure mechanisms of the potential risk zone were non-shear associated with the stress-induced fracturing. Moreover, the wall caved close to the free faces. The temporospatial evolution law of the MS events and analysis of the seismic source parameters could be used to reveal the instability mechanism of the surrounding rock mass, which is a promising method for determining the damage and failure zones due to the excavation-induced unloading.

✉ Jie Xu
besurexj@163.com

1 Geotechnical Research Institute, Hohai University, Nanjing 210098, China

2 Key Laboratory of Ministry of Education for Geomechanics and Embankment Engineering, Hohai University, Nanjing 210098, China

3 Nanjing Hydraulic Research Institute, Nanjing 210029, China

4 School of Civil Engineering, Wuhan University, Wuhan 430072, China

Keywords Stability analysis · Microseismic monitoring · Excavation unloading · Deep-buried caverns

1 Introduction

In recent years, several deep-buried underground projects are being constructed in China. Many studies found that the geological conditions change because of the excavation-unloading effect, usually causing mining damage and geological degradation. The high-intensive excavation process leads to stress redistribution and rapid changes in the stress and strain; moreover, it even induces unstable geological hazards, such as rock bursts, which are a threat to builders and equipment. Hence, the stability of the surrounding rock mass has played a significant role in the safe construction of deep-buried engineering projects [1–3].

In fact, many scholars, domestic and foreign, have investigated the instability mechanism of the surrounding rock mass due to the excavation-induced unloading. Zhu et al. [4,5] proposed a methodology to evaluate the side-wall displacements of underground openings, considering different conditions, whose calculation results were consistent with those obtained using in situ measurements. Sitharam and Latha [6] used a practical, equivalent continuum approach to investigate the properties of jointed rock masses. Yazdani et al. [7] performed a displacement-based numerical back analysis to investigate the properties of the rock mass. The calculated results obtained using the continuum and discontinuum approaches matched well with the measured displacements. Aydan et al. [8] proposed empirical equations to evaluate the damage inflicted to the underground structures during earthquakes. Yoshida and Horii [9], Tezuka and Seoka [10], and Dhawan et al. [11] investigated the excavation response of a large-scale cavern based on the finite

element and discrete-element methods. Zhang et al. [12] presented a method based on the "virtual block" concept, which is a significant improvement over the existing stratified rock-engineering methods. Li et al. [13] investigated the measured results of the surrounding rock due to unloading disturbance, including displacement, excavation damaged zone (EDZ), and deformation convergence. Moreover, they investigated the mechanical behavior of loosened zones, which helped in optimizing the support systems. The aforementioned studies extended the understanding of damage mechanisms and stability assessments of surrounding rock masses. In recent years, in situ measurement methods have been widely used in underground engineering such as multiple position extensometers and microseismic (MS) monitoring techniques. The measurement results reflect the mechanical mechanism of surrounding rock masses due to excavation unloading and provide a reliable basis for the numerical simulation and lab tests.

The MS-monitoring technique is a high-tech and informative dynamic monitoring technique used to detect the micro-fracturing signals of the surrounding rock mass in real time. The technique can be used to capture and record the initiation and propagation of new fractures or existing fractures by analyzing the characteristics of the signal, such as amplitude distribution, energy rate, location, and moment magnitude [14–16]. Consequently, the deformation and failure properties of the rock mass can be assessed and identified based on the information obtained using the MS-monitoring technique. The MS-monitoring technique has come into wide use in many fields, including rock slopes [17,18], underground mining [19–21], deep tunnels [22–25], and generation of electricity using hot dry rocks [26]. According to the temporospatial distribution law of the MS events, Xu et al. [27] studied the dynamic instability process and evaluated the stability of the rock mass due to the unloading disturbance in the Jinping first-stage hydropower station. Gibowicz et al. [28] summarized the studies on seismicity due to excavation, which covered the microseismicity triggering mechanism, prediction and treatment of microseismic events, and improvement in the microseismic monitoring system. By analyzing the MS clusters in a coalmine, Lesniak and Isakow [19] established the relationship between the occurrence times of high-energy tremors and evaluated the hazard function. Chen et al. [29] summarized and investigated the mechanical mechanism of rock bursts by analyzing the MS evolutional laws applied near the rock burst. Hudyma and Potvin [20] proposed a new engineering method to control the seismic risk in hard rock mines. By investigating the MS effects, Lu et al. [21] determined the frequency-spectrum evolutionary rules of MS events before and after a rock burst due to roof falls. However, in the aforementioned studies, the MS-monitoring technique has rarely been applied to evaluate the stability of deep-buried mines with the excavation face advancing.

An MS-monitoring system was installed to round-the-clock monitor the microseismic activities in the 62nd mining area of the Xinzhuangzi Coalmine in this paper. By investigating the temporospatial distribution of the MS events, the potential risk zones were determined. Moreover, the deformation and failure of the potential risk zone were evaluated based on the MS data. The MS parameters, moment magnitude, and E_S/E_P were analyzed. The deformation and failure mechanisms of the surrounding rock mass were then revealed.

2 Engineering Background

2.1 Project Introduction

The Huainan Coalmine, which is approximately 140 km long along the eastwest direction and 20–30 km wide along the southeast direction, is located in the north-central part of Huainan in Anhui, covering an area of approximately 3200 km^2. The main structural trace of the Huainan Coalmine is the largely EW-trending tectonic basin, which lies in the southern margin of the Huabei slab. The imbricate fan of the thrust-nappe structure is developed along the south and north flanks of the tectonic basin. Moreover, a synclinorium with northwest by west is situated in the center of the tectonic basin.

Because of the complexity of the geology conditions and mining procedures, many problems exist in the Huainan Coalmine, such as coal and gas outbursts, rockbursts and gushing water. The Huainan Coalmine is concealed by the Cenozoic loose beds. The coal-bearing strata include the upper carboniferous Taiyuan formation and the Shanxi formation and the lower Shihezi formation and upper Shihezi formation of Permian. The coal seam in the Taiyuan formation is thin and unstable; thus, it is unfit for mining. The total thickness of the Shanxi and Shihezi formations is 755 m, which is divided into seven coal-bearing members. The total thickness of the coal seam is 33.74 m, and the coal-bearing ratio is 4.5%. The mineable coal thickness is 25.1 m.

2.2 In Situ Stress Conditions

The in situ stress measurements were conducted at the depths in the range of −500 to −1000 m in the Huainan Coalmine using a hydraulic- fracturing technique. The analyses of twelve effective measuring data (see Table 1) indicate the following: (1) The in situ stress field in the Huainan Coalmine, wherein the tectonic stress is predominant, is dominated by the horizontal stress and can be classified under the typical tectonic stress field. (2) The maximum principal stress is in

Table 1 In situ stress measurement results using hydraulic-fracturing technique

Position of each measuring point	No.	Z (m)	σ_H (MPa)	σ_h (MPa)	σ_v (MPa)	$\frac{\sigma_H}{\sigma_V}$	$\frac{\sigma_{h,\mathrm{av}}}{\sigma_V}$	Orientation of σ_H (°)
Ventilated roadway about 502 m below sea level in Paner mine	1	502.0	20.85	11.62	11.44	1.81	1.41	84
Connection roadway about 522 m below sea level in Paner mine	2	535.8	20.64	10.84	12.14	1.67	1.28	83
	3	537.8	20.20	10.99	12.36	1.63	1.26	84
52nd cross-hole about 612 m below sea level in Xinzhuangzi mine	4	623.0	15.74	8.19	14.33	1.10	0.84	66
	5	627.0	15.92	8.61	14.42	1.10	0.85	64
	6	629.0	17.00	9.46	14.47	1.18	0.91	65
C_{15} transportation roadway about 820 m below sea level in Wangfenggang mine	7	842.0	20.22	11.78	18.46	1.09	0.86	80
	8	843.3	20.11	11.78	18.52	1.08	0.86	79
	9	844.2	18.67	11.20	18.58	1.01	0.80	81
Shaft station about 960 m below sea level in Wangfenggang mine	10	981.0	24.07	12.38	21.48	1.12	0.84	82
	11	983.2	23.39	12.07	21.63	1.08	0.82	83
	12	984.7	22.68	11.93	21.71	1.05	0.80	83

the range of 19–23 MPa, indicating that the in situ stresses are high. (3) The lateral-pressure coefficient, defined as the ratio of the maximum horizontal principal stress to the vertical principal stress, decreases with the increase in the depth; the in situ stress field changes from dynamic to static. (4) The orientation of the maximum horizontal principal stress is approximately NEE-EW. The relationship between the in situ stress and the tectonics for the Huainan mining area indicated that the orientation of the maximum principal stress was closely related to the tectonic movement, whereas the orientation of the current tectonic stress field is roughly identical with that of the measured maximum horizontal principal stress of the mining area.

3 Excavation-Induced MS Activities

3.1 Principle of MS Monitoring

The MS-monitoring technique is one of the major methods of monitoring the stability of rock masses in underground engineering projects by obtaining the acoustic emission pertaining to the rock- mass fracturing. Studies show that rock masses release the stored energy in the form of acoustic waves for some time before failure. The amount of energy released changes along with the stress states of the rock mass. Each signal contains important information, which reflects the changes in the physico-mechanical conditions in the rock mass. The MS monitoring can be used to capture and record the initiation and propagation of new fractures or existing fractures by analyzing the characteristics of the signal such as amplitude distribution, energy rate, location, and moment magnitude. Consequently, the deformation and failure mechanism of the rock mass can be assessed and identified based on the information obtained using the MS monitoring. In particular, based on the dynamic evolution of the MS events, the potential unstable regions can be identified.

3.2 Determination of Measuring Range

The Xinzhuangzi mine (see Fig. 1) with complex geological conditions is vulnerable to dynamic disaster, particularly in the 62nd mining area. After previous on-site inspection and data analysis, the physico-mechanical properties of the coal and rock in the 62nd mining area were obtained. To monitor the unstable behaviors in the overlying rock strata of C13 and C14 working faces during the mining period, a high-resolution MS monitoring system was employed to

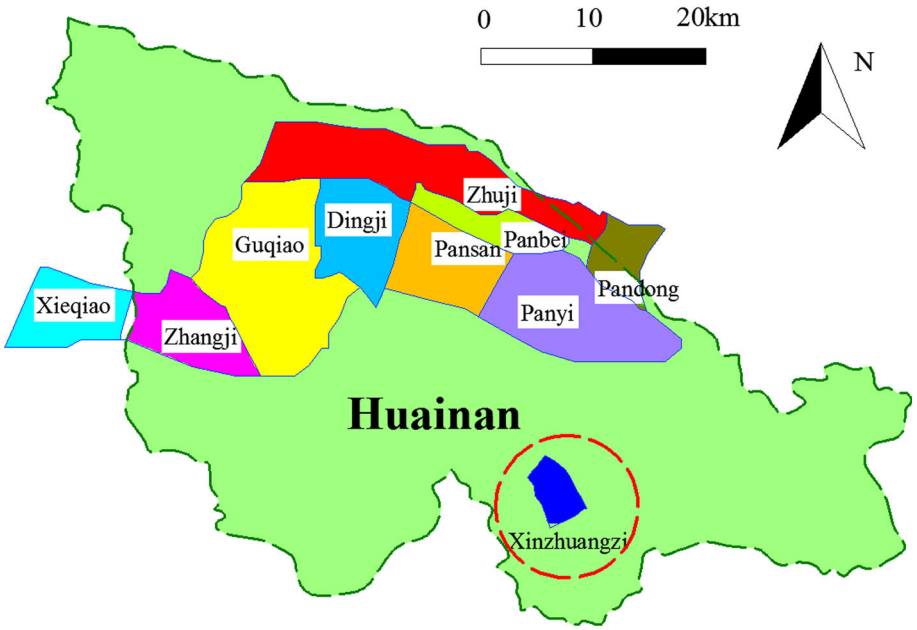

Fig. 1 Location of Xinzhuangzi Mine in Huainan Coalmine

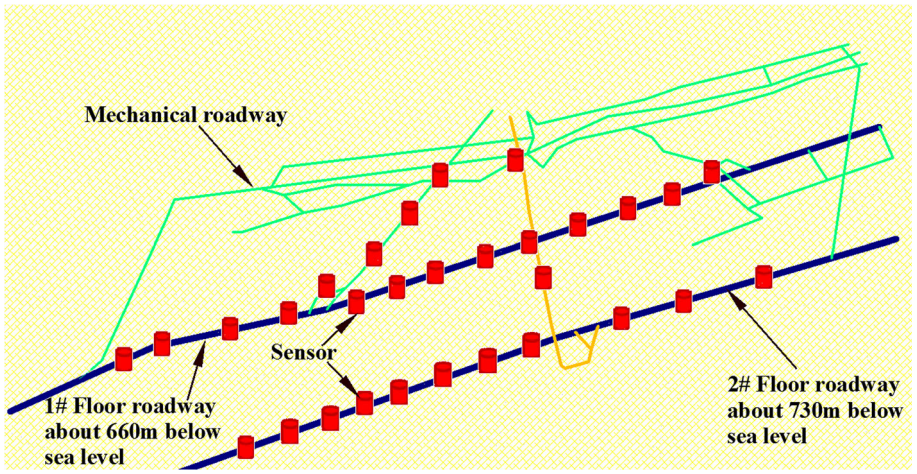

Fig. 2 Sensor arrangement of MS-monitoring system in mining area

round-the-clock monitor the MS activities in the 62nd mining area. The extraction scheme and construction convenience are the major considerations when designating the monitoring areas. After determining the main monitoring areas, the installation layout and arrangement density of the sensors must ensure the optimal MS location and accurate monitoring. Hence, the monitoring areas were selected as follows. Thirty sensors were installed on the floor roadways at a distance of approximately 660 or 730 m below the sea level in the working faces, which formed a three-dimensional monitoring space and covered largely the entire mining area (see Fig. 2).

To ensure accurate and sensitive monitoring, the average distance between adjacent sensors was in the range of 50–120 m, forming a more balanced distribution. Table 2 presents the three-dimensional coordinates of the thirty sensors.

To evaluate the reliability of the sensors, beating experiments were conducted close to the position of the installed sensors. In addition, to obtain the source location error, on-site blasting experiments were conducted. Accordingly, the velocity was measured by conducting seismic-wave velocity experiments. Eleven blasting positions in the working face were determined using the total-station. The wave velocity of the surrounding rock was about 4300 m/s, which was used to set the corresponding parameters in the system to locate the blasting events. Based on the test results, the mean location error was less than 5 m, implying that the accuracy of the MS-monitoring system was high. The triggering threshold of STA/LTA was set as 3 with the intent to filter the noise, whose reasonability was verified after half-a-year applications. The filtered noise events were shown in the data reception window as gray stripes, whereas the MS events or some blasting events appeared blue, as shown in Fig. 3. Figure 4 shows the

Table 2 Three-dimensional coordinates of thirty sensors installed in the mining area

Position	Sensor	X-Northing	Y-Easting	Z-Elv
Floor roadway about 660 m below sea level	1	3600.10	7912.60	−655.70
	2	3643.70	7888.00	−659.70
	3	3691.80	7859.00	−656.30
	4	3738.50	7833.10	−656.80
	9	3842.60	7767.60	−657.50
	10	3881.40	7740.60	−657.40
	11	3926.10	7709.30	−657.90
	12	3979.30	7672.30	−657.80
	13	4028.60	7637.50	−658.30
	14	4115.80	7576.50	−658.70
	15	4150.10	7552.80	−658.30
	16	4170.60	7538.70	−658.10
	17	4242.90	7488.30	−657.40
Floor roadway about 730 m below sea level	20	4334.00	7558.30	−723.90
	21	4262.00	7605.00	−723.90
	22	4226.80	7627.30	−724.40
	23	4109.20	7704.10	−724.40
	24	4047.50	7747.70	−724.10
	25	3979.00	7795.20	−723.80
	26	3932.90	7827.70	−723.50
	27	3890.50	7857.50	−723.10
	28	3854.10	7883.10	−722.70
	29	3814.70	7910.90	−722.50
	30	3752.70	7954.20	−721.80
Mechanical roadway	5	3780.40	7787.40	−657.10
	6	3837.70	7724.10	−640.00
	7	3857.70	7685.50	−629.40
	8	3883.80	7636.00	−614.60
	18	4043.20	7549.70	−637.30
	19	4092.70	7630.30	−680.40

typical waveforms of the MS events. To ensure the location accuracy, four sensors should be triggered to receive the MS signals, which would be converted into MS source parameters such as location information, radiated energy and source radius. Based on the analysis of the MS source parameters, the mechanical mechanism of the surrounding rock can be understood.

3.3 Temporal Distribution of MS Events

The system came into use on May 16. The different properties of the microseismicity including MS events, blasting events, and the noise due to the constructions and machineries were received. Based on the statistics, 2531 effective MS events were recorded after extracting the disturbing signals until October 20. Figure 5 shows the temporal distribution of the MS activities from May 16 to October 20. It was found that approximately 0–50 MS events came about every day with an average of approximately 16 MS events a day. The MS events during the initial excavation period for 1# roadway were relatively quiet, from approximately May 16 to June 16. The sharp increases in the MS events on May 26 and August 19 were primarily induced by the excavation-unloading disturbance. As shown in Fig. 5, the MS signals activated, and the MS events continued to increase until the end of August.

The blasting activities (see Fig. 5) obtained using the monitoring system indicated that the change in the MS events is closely associated with the frequency of the blasting excavation. The more the blasting activity, the more frequent is the MS events. Because of the unloading disturbance, the initial stress balance is low and the internal stress redis-

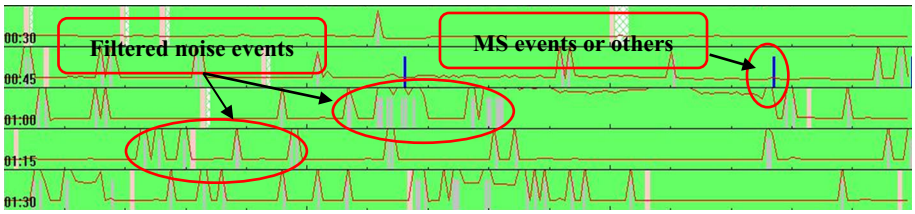

Fig. 3 Process of filtering the noise by setting a triggering threshold of STA/LTA

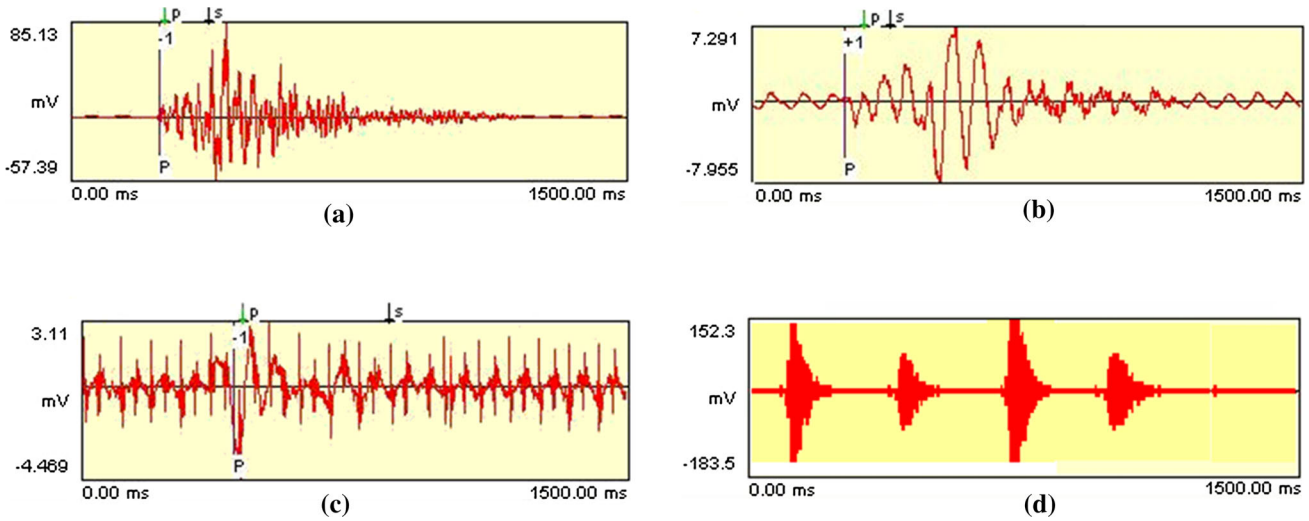

Fig. 4 Typical waveforms for MS events recorded in working face. **a** MS events (large amplitude), **b** MS events (small amplitude), **c** noise events, **d** blasting events

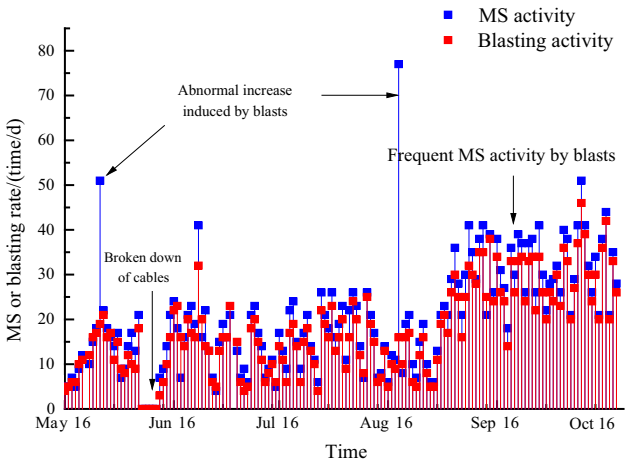

Fig. 5 Temporal distribution of MS activities and blasting activities from May 16 to October 20

tributes, resulting in a local stress concentrated area in the surrounding rock. When the stress and energy concentrated to a certain extent, micro-cracks initiated along with the release of energy, and subsequently, a new stress balance formed. Dai et al. [30] proposed that stress redistribution due to unloading disturbance has a greater effect on MS activities compared with transient excavation impact, which gives further explanations. The continuous increase in the MS events generally resulted from the abrupt change in stress redistribution of the surrounding rock mass due to the blasts. It can be regarded as an onset of unstable failure of rock mass.

3.4 Spatial Distribution of MS Events

The micro-fracture initiation and propagation reflect the stress redistribution and corresponding displacements of the rock mass. Thus, it is significant to localize the micro-fracture location in the rock mass to study the process of rock failure and predict the final failure position. Figure 6 shows the results of the MS monitoring from May 16 to August 11 in the 1# roadway tunneling process. During May 16–31, the micro-fracture clusters began to emerge in both 1# and 2# roadways, and most of the MS events were distributed in a cuboid area, which is 30 m long, 30 m wide, and 50 m tall (see Fig. 6a). As shown in Fig. 6b, the micro-fractures were found to extend along the left of 2# roadway on June 1. Consequently, more MS events gathered in the left close to the connection roadway. During June 16–30, apparent micro-fracture concentration zone shifted to the connection roadway, whereas the MS activities of the other zones were relatively quiet. In the next 15 days, more MS events were detected in the connection roadway, shown in Fig. 6d. However, the continuous excavation of 1# roadway resulted in the transfer of MS events. As shown in Fig. 6e, f, dense

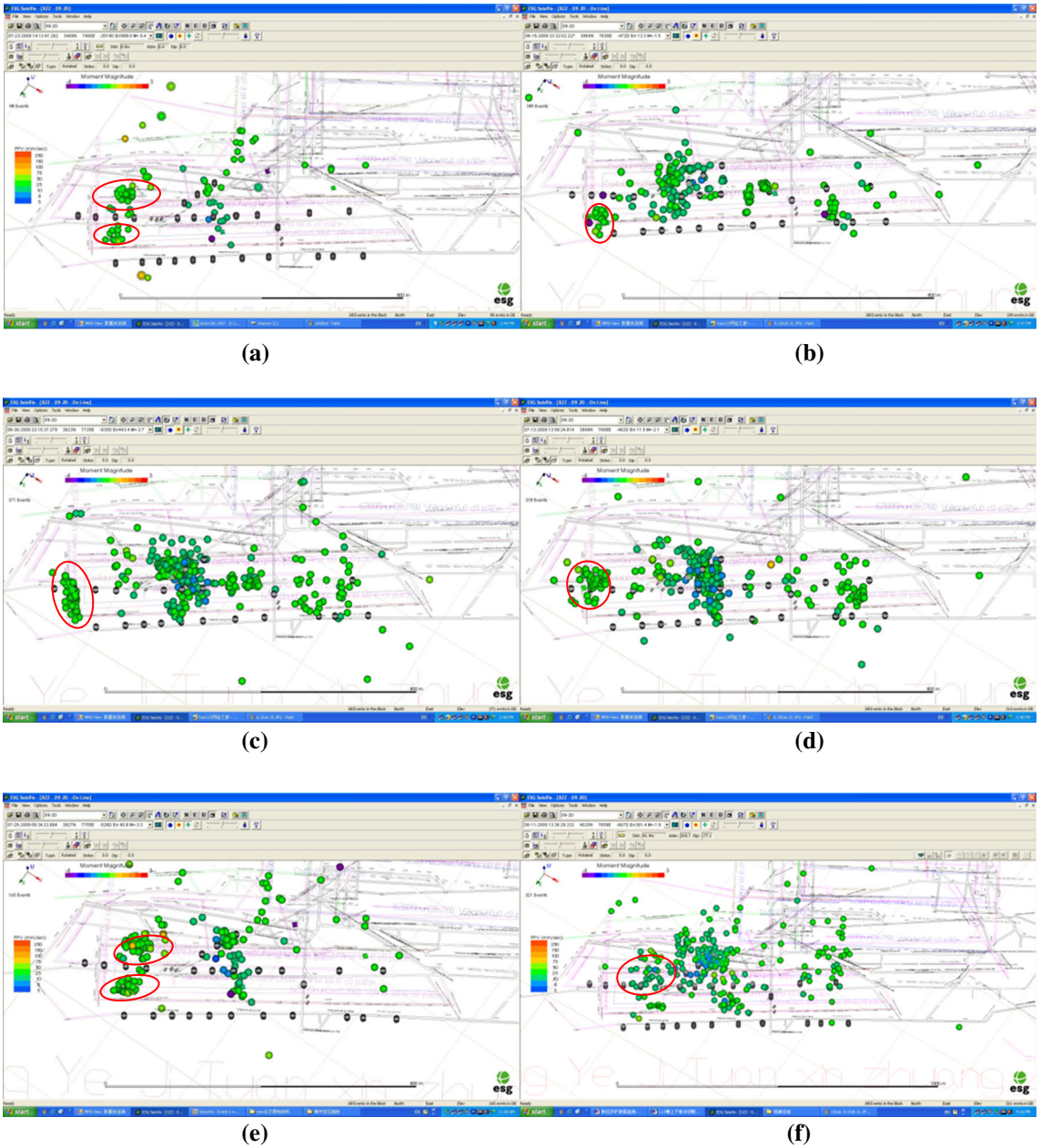

Fig. 6 Accumulation of microseismic events from May 16 to August 11. **a** May 16–31, **b** June 1–15, **c** June 16–30, **d** July 1–15, **e** July 16–31, **f** August 1–11

MS events were captured in 1# and 2# roadways, forming the micro-fracture concentration areas, implying that the MS activities began to enter the active period and more attention needed to be paid.

Figure 7 shows the evolution of a potential risk zone in 2# roadway obtained using the MS monitoring. As shown in Fig. 7a, a significant number of MS events appeared in 2# roadway on 11 August. In the next 15 days, some micro-fractures with large magnitude, amplitude, and energy rate were initiated in 2# roadway, albeit in small amounts. During August 25–September 30, the micro-fractures continued to propagate; thus, the MS events appeared more in this area. Moreover, the amplitude of most of the MS events was above 200 mv, indicating that higher energy was released as the fracture propagated. Consequently, the area in 2# roadway at a distance of 150 m from the connection roadway was determined as the main damage zone in the working face. In this zone, a large number of high-magnitude and high-energy MS events were observed, indicating that the released energy is large in magnitude in the surrounding rock subjected to the unloading disturbance. Based on the theory of energy dissipation, a micro- crack represents a slight damage. As the

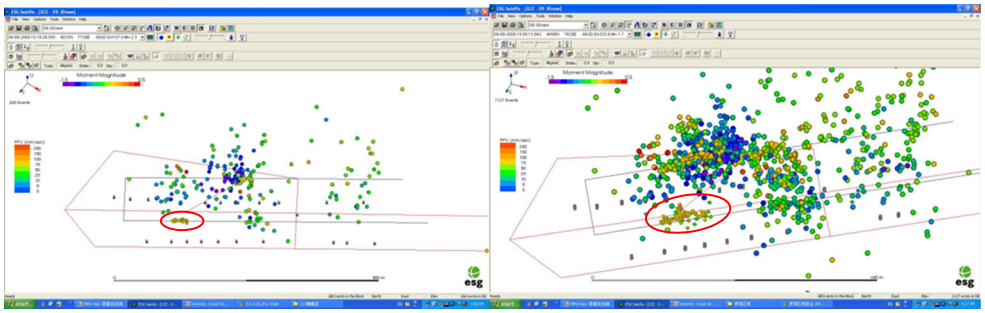

(a) (b)

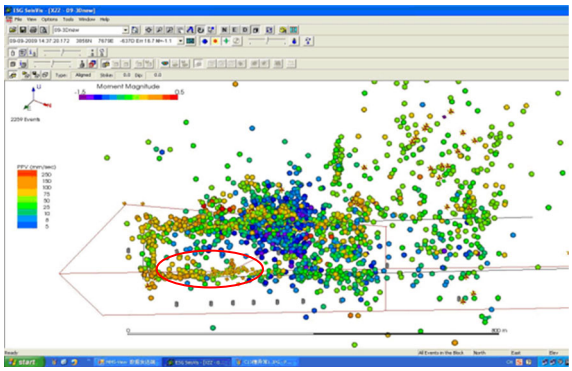

(c)

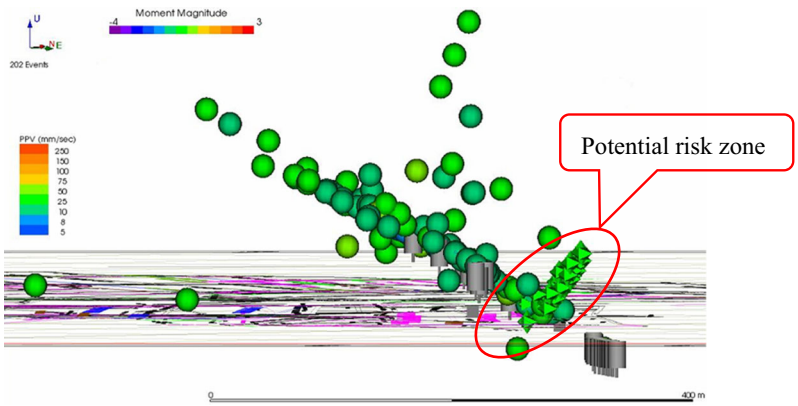

(d)

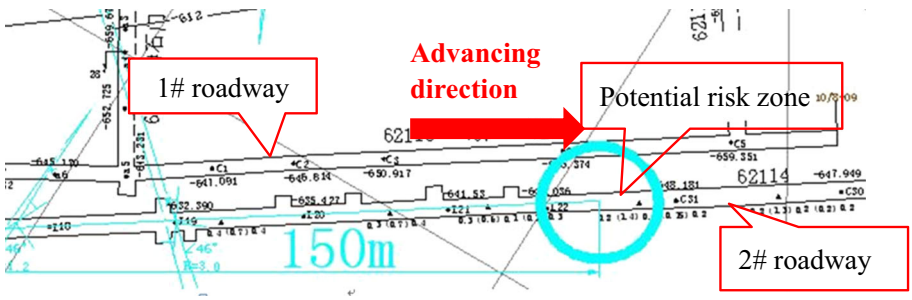

(e)

Fig. 7 Evolution of potential risk zone in 2# roadway obtained using MS monitoring. **a** August 11–25, **b** August 25–September 30, **c** August 11–September 30, **d** sectional drawing of potential risk zone, **e** potential risk zone in the 2# roadway

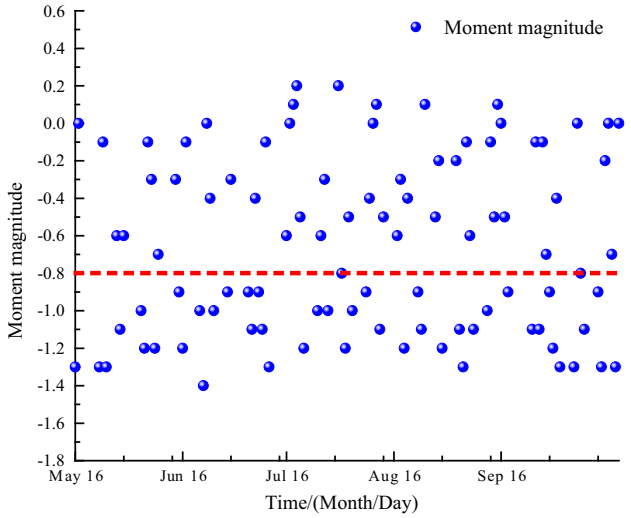

Fig. 8 Distribution chart of moment magnitudes with respect to time in potential risk zone

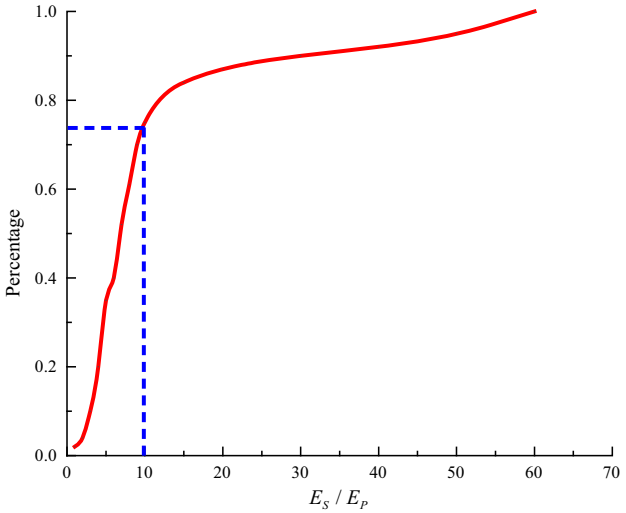

Fig. 9 E_S/E_P curves of MS events in potential risk zone obtained from MS monitoring

damage accumulates, the energy inside the surrounding rock is continuously released, thus decreasing the magnitude of the mechanical parameters and further increasing the damage.

4 Deformation and Failure Forecasting of Potential Risk Zone Based on MS Data

The study found that the MS events were largely concentrated in the specific areas where the surrounding rock mass were prone to failure. The investigation on the activity patterns of the MS event clusters helped in evaluating the damage risks and provided a basis for excavation and support. The deformation and failure assessment of the potential risk zone in the working face were analyzed in this section based on the MS-monitoring signals.

Figure 8 shows the changing process of the moment magnitudes with respect to time in the potential risk zone, as indicated in Fig. 7. The x-axis represents the time during which the MS system was used, whereas the y-axis represents the moment magnitudes of the MS events obtained from the MS system. The moment magnitudes of the MS events recorded in the potential risk zone ranged from -1.4 to 0.3, and 70% of them concentrated in the range of -1.2 to 0.2, which formed a normal distribution with a mean of -0.8. The red line indicates the mean value of the normal distribution, as shown in Fig. 9. The results of the analysis are that the moment magnitudes of the MS events subjected to unloading disturbance were higher, which revealed that more serious damage was induced within the rock mass.

The MS-monitoring system can be used to calculate the energies of the P-wave and S-wave, which were emitted from the seismic source. The energies of the P-wave and S-wave are expressed as E_S and E_P, respectively, whereas E_S/E_P served as an indicator to investigate the mechanical mechanism of the seismic source. Many studies showed the characteristics of the P-wave and S-wave and the difference between them. Gibowicz et al. [31] showed that more energy was induced in the S-wave from the MS events than that in the P-wave when the fault slip occurred. E_S/E_P higher than 10 represented the fault-slip mechanism and closer to 3 revealed the non-shear mechanism including the tensile failure and stress-induced fracturing, which was proposed by Boatwright and Fletcher [32]. A similar conclusion was obtained by Gibowicz and Kijko [33] based on the calculation using an equation. When evaluating the fracture size combined with a tensile model, Cai et al. [34] concluded that approximately 78% of the 804 events had E_S/E_P less than 10, which was consistent with the in situ tensile failure. Based on the above studies, $E_S/E_P$was also used to assess the deformation and failure mechanism in the potential risk zone. Figure 9 shows the E_S/E_P curves of the MS events in the potential risk zone obtained from the MS monitoring. It was found that approximately 74% of the MS events in the potential risk zone had an E_S/E_P value of below 10, indicating that the deformation and failure mechanisms were non-shear associated with the stress-induced fracturing due to the blasting excavation. After excavating the underground caverns, the surrounding rock before reinforcement near the free face has no horizontal pressure, which is more likely to undergo tensile damage due to the vertical principle stress. Numerical studies [35] and in situ measurements [36,37] indicate that the adjustment of stress is complicated, including stress increase and decrease and stress rotation. The frequent unloading effect gives rise to constant adjust-

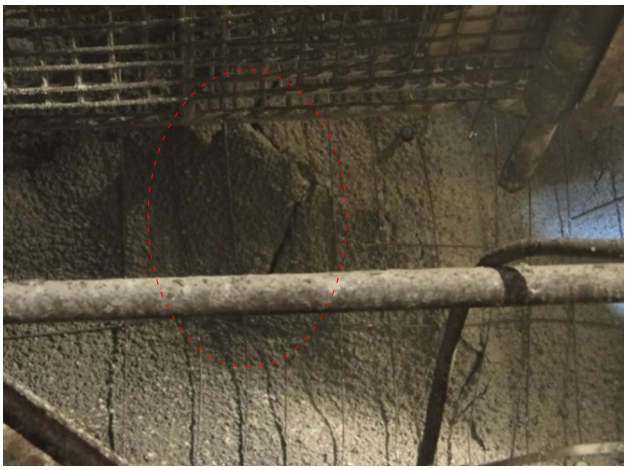

Fig. 10 Cracking occurs in potential risk zone obtained using MS monitoring

ment of the local stress, causing a significant number of small tensile fractures with low magnitude and low energy.

Based on the analysis of the seismic characteristics of the MS events, the failure mode of the surrounding rock mass in the potential risk zone was revealed. As shown in Fig. 10, the cracking occurred in this zone because of excavation disturbance. Some studies presented that even small tangential stress will give rise to the fracture of surrounding rock subjected to unloading disturbance [38,39]. A lot of new cracks propagate and ran through in the process of stress adjustment, eventually leading to a macroscopic failure. The failure risk control of the roadways excavated by drilling and blasting methods involves modifying the shape of the roadway face and reducing the blasting circulation measurement, or employing a stress release method to reduce the stress concentration of the surrounding rock. In addition, it is important to enhance the impact-resistant ability of the surrounding rock to select high-quality supporting structure system. The conventional rigid anchor bolts often exhibit tensile failure and, hence, are unable to adapt to large deformations of the surrounding rock. A type of anchor bolt with constant resistance and large deformation can be used to effectively control damage risks. The reason is that this system comprises a constant resistance device and an elastic rod, which help in providing a constant resistance and stable deformation.

5 Conclusions

The MS-monitoring system was implemented in the Huainan Coalmine, which was used to monitor in real time and evaluate the stability of the surrounding rock mass in the working face. According to the temporal distribution of the MS events obtained using the MS monitoring system, it was found that the MS activities were strongly influenced by the excavation unloading. The sharp increase in the MS events occurred at the end of August, resulting from an abrupt change in the stress or stress redistribution of the surrounding rock mass subject to excavation. This behavior can be regarded as an onset of instable failure of the rock mass.

The micro-fracture initiation and propagation reflect the stress redistribution and corresponding displacements of the rock mass. Thus, it is significant to localize the micro-fracture location in the rock mass to study the process of the rock failure and predict the final failure position. Based on the results of the MS monitoring, the spatial distribution of the MS events was obtained. The results indicated that the micro-fractures continued to propagate; thus, the MS events concentrated in an area in 2# roadway from August 25, which was at a distance of 150 m from the connection roadway. The potential risk zone in the working face was determined using the MS-monitoring technique.

The deformation and failure forecasting of the potential risk zone was conducted based on the MS data. The MS parameters, moment magnitude, and E_S/E_P were analyzed. The results indicated that a more serious damage was induced within the rock mass because of the excavation-induced unloading. Moreover, the deformation and failure mechanisms were non-shear associated with the stress-induced fracturing. Thus, the key measures, such as anchoring and shotcreting and hanging steel bar meshes, should be implemented to control the main potential risks.

Acknowledgements This work was supported by China Postdoctoral Science Foundation (Grant No. 2017M611676), the National Natural Science Foundation of China (Grant No. 41630638), the National Key Basic Research Program of China ("973" Program) (Grant No. 2015CB057901), the Public Service Sector R&D Project of Ministry of Water Resource of China (Grant No. 201501035-03), "333" Projects of Jiangsu Province (Grant No. BRA2015312), and the 111 Projects (Grant No. B13024).

References

1. Young, R.P.: Rockbursts and Seismicity in Mines. A.A, Balkema, Canada (1993)
2. Tang, C.A.; Wang, J.M.: Rock and seismic monitoring and prediction-the feasibility and the preliminary practice. Rock Mech. Eng. News **89**(1), 43–55 (2010)
3. Yu, H.T.; Chen, J.T.; Bobet, A.; Yuan, Y.: Damage observation and assessment of the Longxi tunnel during the Wenchuan earthquake. Tunn. Undergr. Space Technol. **54**, 102–116 (2016)
4. Zhu, W.S.; Sui, B.; Li, X.J.; Li, S.C.; Wang, W.T.: A methodology for studying the high wall displacement of large scale underground cavern groups and it's applications. Tunn. Undergr. Space Technol. **6**, 651–664 (2008)
5. Zhu, W.S.; Li, X.J.; Zhang, Q.B.; Zheng, W.H.; Xin, X.L.; Sun, A.H.; Li, S.C.: A study on sidewall displacement prediction and stability evaluations for large underground power station caverns. Int. J. Rock Mech. Min. Sci. **47**(7), 1055–1062 (2010)
6. Sitharam, T.G.; Latha, G.M.: Simulation of excavations in jointed rock mass using a practical equivalent continuum approach. Int. J. Rock Mech. Min. Sci. **39**, 517–525 (2002)

7. Yazdani, M.; Sharifzadeh, M.; Kamrani, K.; Ghorbani, M.: Displacement-based numerical back analysis for estimation of rock mass parameters in Siah Bisheh powerhouse cavern using continuum and discontinuum approach. Tunn. Undergr. Space Technol. **28**, 41–48 (2012)
8. Aydan, Ö.; Ohta, Y.; Geniş, M.; Tokashiki, N.; Ohkubo, K.: Response and stability of underground structures in rock mass during earthquakes. Rock Mech. Rock Eng. **43**(6), 857–875 (2010)
9. Yoshida, H.; Horii, H.: Micromechanics-based continuum model for a jointed rock mass and excavation analyses of a large-scale cavern. Int. J. Rock Mech. Min. Sci. **41**, 119–145 (2004)
10. Tezuka, M.; Seoka, T.: Latest technology of underground rock cavern excavation in Japan. Tunn. Undergr. Space Technol. **18**, 127–44 (2003)
11. Dhawan, K.R.; Singh, D.N.; Gupta, I.D.: Three-dimensional finite element analysis of underground caverns. Int. J. Geomech. **4**, 224–228 (2004)
12. Zhang, Z.X.; Xu, Y.; Kulatilake, P.H.S.W.; Huang, X.: Physical model test and numerical analysis on the behavior of stratified rock masses during underground excavation. Int. J. Rock Mech. Min. Sci. **49**, 134–147 (2012)
13. Li, S.J.; Yu, H.; Liu, Y.X.; Wu, F.J.: Results from in-situ monitoring of displacement, bolt load, and disturbed zone of a powerhouse cavern during excavation process. Int. J. Rock Mech. Min. Sci. **45**, 1519–1525 (2008)
14. Potvin, Y.; Hudyma, M.R.: Keynote address: seismic monitoring in highly mechanized hardrock mines in Canada and Australia. In: van Aswegen, G., Durrheim, R.J., Ortleep, D.D. (eds.) Proceedings of Fifth International Symposium on Rockburst and Seismicity in Mines, pp. 267–280. The South African Institute of Mining and Metallurgy, Johannesburg (2001)
15. Ma, T.H.; Tang, C.A.; Tang, L.X.; et al.: Rockburst characteristics and microseismic monitoring of deep-buried tunnels for Jinping II Hydropower Station. Tunn. Undergr. Space Technol. **49**, 345–368 (2015)
16. Dai, F.; Li, B.; Xu, N.; et al.: Deformation forecasting and stability analysis of large-scale underground powerhouse caverns from microseismic monitoring. Int. J. Rock Mech. Min. Sci. **86**, 269–281 (2016)
17. Lynch, R.A.; Wuite, R.; Smith, B.S.; Cichowicz, A.: Micro-seismic monitoring of open pit slopes. In: Potvin, Y.; Hudyma, M. (eds.) Micro-seismic Monitoring of Open Pit Slopes. Proceeding of the 6th Symposium on Rockbursts and Seismicity in Mines, pp. 581–592. ACG, Perth, Australia (2005)
18. Xu, N.W.; Dai, F.; Liang, Z.Z.; Zhou, Z.; Sha, C.; Tang, C.A.: The dynamic evaluation of rock slope stability considering the effects of microseismic damage. Rock Mech. Rock Eng. **47**, 621–642 (2014)
19. Lesniak, A.; Isakow, Z.: Space-time clustering of seismic events and hazard assessment in the Zabrze-Bielszowice coal mine, Poland. Int. J. Rock Mech. Min. Sci. **46**, 918–928 (2009)
20. Hudyma, M.; Potvin, Y.H.: An engineering approach to seismic risk management in hardrock mines. Rock Mech. Rock Eng. **43**, 891–906 (2010)
21. Lu, C.P.; Dou, L.M.; Zhang, N.; Xue, J.H.; Wang, X.N.; Liu, H.; Zhang, J.W.: Microseismic frequency-spectrum evolutionary rule of rockburst triggered by roof fall. Int. J. Rock Mech. Min. Sci. **64**, 6–16 (2013)
22. Tang, C.A.; Wang, J.M.; Zhang, J.J.: Preliminary engineering application of microseismic monitoring technique to rockburst prediction in tunneling of Jinping II project. J. Rock Mech. Geotech. Eng. **2**(3), 193–208 (2011)
23. Hirata, A.; Kameoka, Y.; Hirano, T.: Safety management based on detection of possible rock bursts by AE monitoring during tunnel excavation. Rock Mech. Rock Eng. **40**(6), 563–576 (2007)
24. Feng, X.T.; Chen, B.R.; Li, S.J.; Zhang, C.Q.; Xiao, Y.X.; Feng, G.L.; Zhou, H.; Qiu, S.L.; Zhao, Z.N.; Yu, Y.; Chen, D.F.; Ming, H.J.: Studies on the evolution process of rockbursts in deep tunnels. J. Rock Mech. Geotech. Eng. **4**(4), 289–295 (2012)
25. Yu, H.T.; Chen, J.T.; Yuan, Y.; Zhao, X.: Seismic damage of mountain tunnels during the 5.12 Wenchan earthquake. J. Mt. Sci. **13**(11), 1958–1972 (2016)
26. Tezuka, K.; Niitsuma, H.: Stress estimated using microseismic clusters and its relationship to the fracture system of the Hijiori hot dry rock reservoir. Eng. Geol. **56**, 47–62 (2000)
27. Xu, S.X.: Design, construction and testing results of the type-581 seismograph. Acta Geophys. Sin. **8**(2), 109–122 (1959)
28. Gibowicz, S.J.: Seismicity induced by mining. Adv. Geophys. **32**, 1–74 (1990)
29. Chen, B.R.; Feng, X.T.; Li, Q.P.; Luo, R.Z.; Li, S.J.: Rock burst intensity classification based on the radiated energy with damage intensity at Jinping II hydropower station, China. Rock Mech. Rock Eng. **48**(1), 289–303 (2015)
30. Dai, F.; Li, B.; Xu, N.W.; Fan, Y.L.; Zhang, C.Q.: Deformation forecasting and stability analysis of large-scale underground powerhouse caverns from microseismic monitoring. Int. J. Rock Mech. Min. Sci. **86**, 269–281 (2016)
31. Gibowicz, S.J.; Young, R.P.; Talebi, S.; Rawlence, D.J.: Source parameters of seismic events at the Underground Research Laboratory in Manitoba, Canada: scaling relations for events with moment magnitude smaller than-2. Bull. Seismol. Soc. Am. **81**, 1157–1182 (1991)
32. Boatwright, J.; Fletcher, J.B.: The partition of radiated energy between P and S waves. Bull. Seismol. Soc. Am. **74**(2), 361–376 (1984)
33. Gibowicz, S.J.; Kijko, A.: An Introduction to Mining Seismology, 1st edn. Academic Press, SanDiego (1994). 396
34. Cai, M.; Kaiser, P.K.; Martin, C.D.: A tensile model for the interpretation of micro-seismic events near underground openings. Pure Appl. Geophys. **153**, 67–92 (1998)
35. Zhang, C.Q.; Zhou, H.; Feng, X.T.: An index for estimating the stability of brittle surrounding rock mass: FAI and its engineering application. Rock Mech. Rock Eng. **44**, 401–414 (2011)
36. Martin, C.D.: Seventeenth Canadian geotechnical colloquium: the effect of cohesion loss and stress path on brittle rock strength. Can. Geotech. J. **34**, 698–725 (1997)
37. Kaiser, P.K.; Yazici, S.; Maloney, S.: Mining-induced stress change and consequences of stress path on excavation stability—a case study. Int. J. Rock Mech. Min. Sci. **38**, 167–180 (2001)
38. Haimson, B.; Chang, C.: A new true triaxial cell for testing mechanical properties of rock, and its use to determine rock strength and deformability of Westerly granite. Int. J. Rock Mech. Min. Sci. **37**, 285–296 (2000)
39. Cai, M.; Kaiser, P.K.; Tasaka, Y.; et al.: Generalized crack initiation and crack damage stress thresholds of brittle rock masses near underground excavations. Int. J. Rock Mech. Min. Sci. **41**, 833–847 (2004)